AGU PUBLICATIONS

JGR

Journal of Geophysical Research: Oceans

RESEARCH ARTICLE

10.1002/2014JC010301

Key Points:
- Observations showed parcels of water in the eddy were entrained from the shelf
- Particle tracking quantified the volume and origin of the entrained waters
- Frontal eddies play a significant role, providing habitat for larval fish

Correspondence to:
J. D. Everett,
jason.everett@unsw.edu.au

Citation:
Everett, J. D., H. Macdonald, M. E. Baird, J. Humphries, M. Roughan, and I. M. Suthers (2015), Cyclonic entrainment of preconditioned shelf waters into a frontal eddy, *J. Geophys. Res. Oceans*, *120*, 677–691, doi:10.1002/2014JC010301.

Received 13 JUL 2014
Accepted 7 JAN 2015
Accepted article online 14 JAN 2015
Published online 5 FEB 2015

Cyclonic entrainment of preconditioned shelf waters into a frontal eddy

J. D. Everett[1,2,3], H. Macdonald[4,5], M. E. Baird[6], J. Humphries[1,2], M. Roughan[2,5], and I. M. Suthers[1,2]

[1]Evolution & Ecology Research Centre, University of New South Wales, Sydney, New South Wales, Australia, [2]Sydney Institute of Marine Science, Mosman, New South Wales, Australia, [3]Plant Functional Biology and Climate Change Cluster, University of Technology Sydney, Sydney, New South Wales, Australia, [4]School of Environmental Systems Engineering, University of Western Australia, Crawley, Western Australia, Australia, [5]Coastal and Regional Oceanography Laboratory, School of Mathematics and Statistics, University of New South Wales, Sydney, New South Wales, Australia, [6]CSIRO Marine and Atmospheric Research, Hobart, Tasmania, Australia

Abstract The volume transport of nutrient-rich continental shelf water into a cyclonic frontal eddy (entrainment) was examined from satellite observations, a Slocum glider and numerical simulation outputs. Within the frontal eddy, parcels of water with temperature/salinity signatures of the continental shelf (18–19°C and >35.5, respectively) were recorded. The distribution of patches of shelf water observed within the eddy was consistent with the spiral pattern shown within the numerical simulations. A numerical dye tracer experiment showed that the surface waters (≤50 m depth) of the frontal eddy are almost entirely (≥95%) shelf waters. Particle tracking experiments showed that water was drawn into the eddy from over 4° of latitude (30–34.5°S). Consistent with the glider observations, the modeled particles entrained into the eddy sunk relative to their initial position. Particles released south of 33°S, where the waters are cooler and denser, sunk 34 m deeper than their release position. Distance to the shelf was a critical factor in determining the volume of shelf water entrained into the eddy. Entrainment reduced to 0.23 Sv when the eddy was furthest from the shelf, compared to 0.61 Sv when the eddy was within 10 km of the shelf. From a biological perspective, quantifying the entrainment of shelf water into frontal eddies is important, as it is thought to play a significant role in providing an offshore nursery habitat for coastally spawned larval fish.

1. Introduction

Frontal eddies are cyclonic eddies that regularly characterize the landward side of all western boundary currents, e.g., Gulf Stream [*Glenn and Ebbesmeyer*, 1994] and the East Australian Current [*Everett et al.*, 2011], and eastern boundary currents, e.g., California Current [*Kim et al.*, 2011] and Benguela Current [*Shannon et al.*, 1984]. These frontal eddies are formed as a result of velocity shear between the current and the continental shelf, or from meanders and instabilities in the boundary current. They range in size from ≈ 10km [*Lee*, 1975] to >100 km diameter [*Nakata et al.*, 2000; *Sponaugle et al.*, 2005].

Frontal eddies generate enhanced primary productivity both within the eddy [*Kimura et al.*, 1997] and on the adjacent continental shelf [*Yoder et al.*, 1981]. They also provide a frequent mechanism for the transport of nutrients across boundary currents such as the Gulf Stream [*Glenn and Ebbesmeyer*, 1994]. Production within frontal eddies is sustained by the shoaling of the nutricline [*Everett et al.*, 2011; *Lee et al.*, 1991], and can result in increased biomass of zooplankton [*Everett et al.*, 2011; *Okazaki et al.*, 2002] and larval fish [*Mullaney and Suthers*, 2013]. Due to their proximity to the coast, frontal eddies may additionally provide an offshore nursery habitat for coastally spawned larval fish [*Govoni et al.*, 2010]. Fish larvae associated with frontal eddies tend to occur in higher concentrations [*Okazaki et al.*, 2002] and have significantly higher abundance of late stage larvae (i.e., survivors) than those from nearby inshore waters [*Logerwell and Smith*, 2001; *Mullaney and Suthers*, 2013]. The presence of coastally spawned larval fish in frontal eddies [*Matis et al.*, 2014; *Mullaney and Suthers*, 2013] suggests the entrainment of water which originated on the continental shelf (shelf water) has occurred, however there is little information on the timing of, or volumes of shelf water entrained into frontal eddies.

The entrainment of particles (plankton and fish) into frontal eddies is rarely observed directly [*Govoni et al.*, 2013] nor the volume quantified. Instead, the entrainment of coastal water into frontal eddies is often

inferred from the abundance of coastal species within the eddy. In the Enshu-Nada Sea off Japan, for example, coastally spawned anchovy eggs and larvae were sampled within a frontal eddy of the Kuroshio Current [*Okazaki et al*., 2002], however the process of larval entrainment was not directly observed. Similarly, entrainment into frontal eddies of the East Australian Current [*Mullaney and Suthers*, 2013; *Matis et al*., 2014] was inferred from the abundance of shelf species sampled within the eddy, rather than observations of the fish being entrained. *Okazaki et al*. [2002] concluded that the physical mechanism behind the entrainment of plankton into frontal eddies is only poorly understood and further investigation of the processes are necessary. In this study, we observe and model the entrainment of continental shelf into a frontal eddy of the East Australian Current, before the entrained water moves further offshore within the eddy.

1.1. Frontal Eddies of the East Australian Current

The East Australian Current (EAC) drives a region of high eddy activity (Eddy Avenue), adjacent to the shelf where the density of cyclonic (clockwise in the southern hemisphere) and anticyclonic eddies (anticlockwise) is at least 16% higher than the average Tasman Sea eddy abundance [*Everett et al*., 2012]. The cyclonic eddies in Eddy Avenue exhibited higher chlorophyll *a* concentrations than those in the rest of the Tasman Sea. One likely mechanism to account for the higher chlorophyll *a* is the entrainment of continental shelf waters which are preconditioned with elevated nutrients [*Roughan and Middleton*, 2002] and phytoplankton [*Armbrecht et al*., 2014; *Everett et al*., 2014] due to the persistent upwelling generated by the EAC flow [*Schaeffer et al*., 2013]. In addition to the larger mesoscale eddy activity ($\gtrsim$80 km), the EAC regularly generates smaller frontal eddies [*Everett et al*., 2011; *Mullaney and Suthers*, 2013], although their abundances have not been measured, nor their entrainment potential quantified.

The formation of a small mesoscale frontal eddy ($\approx$50 km diameter) within the EAC region in October 2009 was reproduced in a numerical modeling simulation [*Macdonald*, 2012]. The model was initialized without a surface signature of the eddy yet the model still formed an eddy similar to that observed without assistance from data assimilation. This means that the modeled fields can be used to study processes in the lead up to eddy formation. The eddy formed in the region where the EAC separates from the coast. This region has a large relative shear between the EAC and the northward flowing counter current on the shelf, providing the energy for eddy formation [*Macdonald*, 2012]. *Macdonald* [2012] examined the energy transfer from the velocity and wind fields during the initial formation of the eddy, and showed the frontal eddy grew by entraining negative vorticity water from the shelf into its center.

In this present study, we rerun the model simulations using numerical tracers and examine in situ observations of entrainment in order to quantify the rate of entrainment of coastal water into the frontal eddy. Our specific aims were to (1) examine the entrainment of enriched shelf water into a frontal eddy using an autonomous glider and satellite observations; and (2) quantify the volume and origin of entrained shelf water using ocean observations and particle and dye tracers within a high-resolution hydrodynamic model. With an improved understanding of the offshore entrainment of coastal water, we can then assess the potential for frontal eddies to provide an offshore nursery ground for coastally spawned larval fish.

2. Methods

2.1. Glider Deployment

The Slocum glider is an autonomous underwater vehicle that uses changes in buoyancy to move in a sawtooth trajectory with a forward velocity of 0.25–0.4 m s^{-1}. The glider was deployed off Crowdy Head (31.85°S 152.76°E) on the southeast Australian coast on 2 October 2009 and retrieved on 19 October 2009 (Figure 1). The glider undulated between the surface and 180 m, depth permitting. After crossing the shelf, the glider path was primarily determined by the ambient current which advected it south. The glider was steered toward the center of the eddy from deployment until 17 October and then away from the center until recovery. This produced a track that spiraled close to the center of the eddy and then back to the perimeter (Figure 1).

The glider sensors included a Seabird-CTD, a WETLabs BBFL2SLO 3 parameter optical sensor (measuring chlorophyll *a*, colored dissolved organic matter (CDOM) and backscatter at 660 nm) and an Aanderaa oxygen optode. CDOM and backscatter are not presented here. The effect of thermal lag on the calculations of

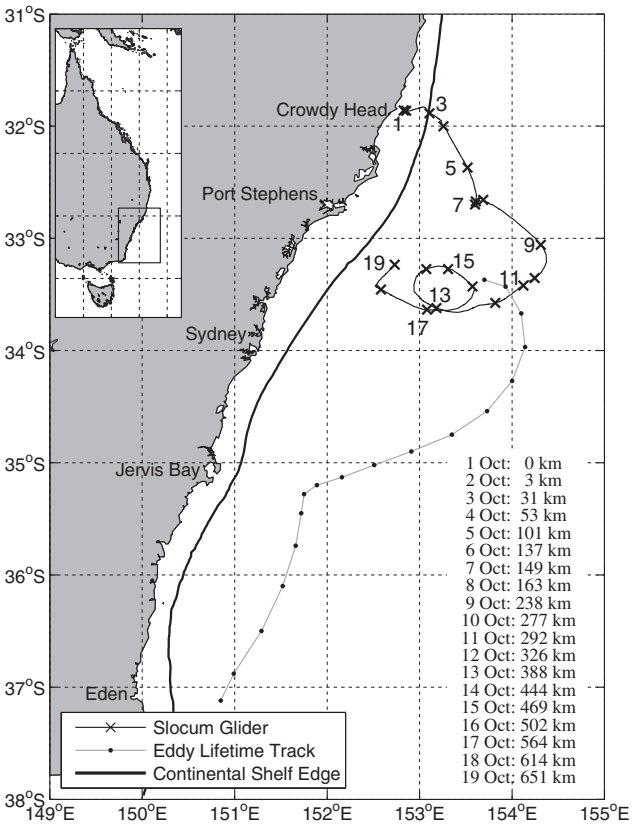

Figure 1. Map of the study area showing the Slocum Glider track (black line with crosses) and the lifetime track of the eddy (gray line with circles; *Chelton et al*. [2011]). The thick black line indicates the 200 m depth contour. The numbers and crosses along the glider track correspond to the location of the glider on the day in October 2009 (1 represents the 00:00 h on 1 October 2009). The corresponding distance along the track is included in the bottom right corner of the figure for comparison with Figure 4. The dots of the eddy lifetime track represent the weekly location of the eddy.

salinity from conductivity, and the effect of nonphotochemical quenching on fluorescence at high light intensities were corrected as per the methods of *Baird et al*. [2011].

2.2. Remotely Sensed Observations

MODIS Level 3 surface ocean color data (chlorophyll *a*) was obtained from the Integrated Marine Observing System (IMOS) Data Portal (http://imos.aodn.org.au/imos/) at 1 km resolution using the OC3 algorithm. Satellite altimeter data were obtained from NASA/CNES (Jason-1 and 2) and ESA (ENVISAT) and mapped in near-real time for the Australian region as described by *Deng et al*. [2011].

Additionally, the lifetime properties of the eddy (location, radii, and rotational speed) are extracted from a publicly available global census of eddies derived from Sea Level Anomaly (SLA) fields [*Chelton et al*., 2011]. Due to the filtering of the SLA fields, eddies of diameter $<$80 km are generally not resolvable and hence this particular eddy is not resolved in the census until it is 7 days old (Table 1). For a full discussion of the methods used to identify and track eddies see *Chelton et al*. [2011].

2.3. Numerical Simulations

The ocean state of the October 2009 cyclonic frontal eddy was simulated using the Regional Ocean Modeling System (ROMS). ROMS solves the primitive nonlinear Boussinesq and hydrostatic equations allowing for a free surface on a curvilinear, terrain-following grid [*Shchepetkin and McWilliams*, 2003, 2005]. For computational efficiency, ROMS uses a split-explicit scheme with a smaller time step for computing the two-dimensional (barotropic) depth integrated continuity and momentum equations than that used for the three-dimensional (baroclinic) momentum and tracer equations. A detailed description of the model's configuration for the EAC region can be found in *Macdonald* [2012] and a brief summary is included here.

The baroclinic time step is set to 60 s and the barotropic time step is 1 s. The *Mellor and Yamada* [1982] 2.5 turbulent closure scheme is used in parameterizing vertical mixing. The grid spacing is approximately 1.75 km by 2.15 km and there are 50 vertical layers. A synthetic vertical temperature and salinity product derived from in situ data (SynTS) [*Ridgway et al*., 2008] is used to prescribe initial and boundary conditions. The *Flather* [1976] condition is applied to the barotropic velocity components at the northern boundary. The baroclinic velocity field and the tracers on the northern boundary use an adaptive nudging scheme [*Marchesiello et al*., 2001] to external estimates from SynTS at a timescale of 4 days. All other boundaries are radiative. The model is forced with winds from the NOAA/NCDC Blended 6 hourly 0.25° Sea Surface Winds data set [*Zhang et al*., 2006]. The model is initialized on 18 September 2009 and, as SynTS is already in

Table 1. The Physical Characteristics of the Cyclonic Eddy Through Time, as Derived From a Global Census of Eddies [*Chelton et al.*, 2011][a]

Date	Latitude	Eddy Speed (km d^{-1})	Eddy Radius (km)	Distance to Shelf (km)	Tangential Velocity (cm s^{-1})
7 Oct 2009	−33.37		85	30	41
14 Oct 2009	−33.43	3	75	62	58
21 Oct 2009	−33.67	4	87	78	65
28 Oct 2009	−33.97	5	111	76	62
4 Nov 2009	−34.27	5	97	101	54
11 Nov 2009	−34.54	6	97	102	56
18 Nov 2009	−34.75	6	84	99	61
25 Nov 2009	−34.9	6	113	44	60
2 Dec 2009	−35.02	6	94	35	50
9 Dec 2009	−35.13	5	68	32	48
16 Dec 2009	−35.2	4	68	10	44
23 Dec 2009	−35.28	2	60	8	41
30 Dec 2009	−35.45	3	53	21	33
6 Jan 2010	−35.74	5	51	34	36
13 Jan 2010	−36.1	6	63	30	37
20 Jan 2010	−36.5	7	61	28	54
27 Jan 2010	−36.88	7	58	3	47
3 Feb 2010	−37.12	4	59	−13	41

[a]The census is based upon altimetry and therefore the eddy does not become visible to the eddy tracking algorithm for approximately 1 week after formation. Eddy speed is the translational speed at which the eddy is moving along the coast (km d^{-1}). Tangential velocity is the velocity at the outermost closed contour.

geostrophic balance, has a short 5 day spin-up. More details on the forcings and initial conditions can be found in *Macdonald* [2012].

Eddy surface area was calculated as the area enclosed by the −0.85 m sea level contour. The distance to the shelf was calculated as the distance from the eddy center to the 200 m isobath. In order to quantify the entrainment process, the model is seeded with both individual particles (as a proxy for plankton or larval fish) and a dye tracer in order to quantify volume of water entrained. In this study, we define "entrainment" as the volume transport across the perimeter of the eddy. The Rossby Number (*Ro*) was calculated as:

$$Ro = \frac{V_t}{D \times |f|} \tag{1}$$

where V_t is the tangential velocity and D is the eddy diameter. The Coriolis Frequency (f) is calculated as $2\Omega \sin \phi$, where Ω is angular frequency of planetary rotation and ϕ is the latitude of the eddy.

2.3.1. Particle Tracking Experiments

Lagrangian particles were released on the 22 September on the continental shelf (areas with a depth <200 m) between 31°S and 34°S. They were released at 0.3° intervals in the latitudinal direction, 0.01° intervals in the longitudinal direction at depths of 0 and 50 m. These depths were chosen to be representative of the euphotic zone, where much of the biological activity occurs. A total of 865 and 846 particles were released at 0 and 50 m depth, respectively. The particles were advected within the model using the modeled velocity field (for u, v, and w). Model velocity was interpolated onto the particle position and particle positions were updated at every time step (60 s). Random walk processes were not included as experiments show these are not critical to the results over the short timeframe of the simulations. The particles that were entrained into the eddy were counted and their tracks used to quantify the location and timing of entrainment.

2.3.2. Dye Tracer Experiments

Passive tracers can be released into this configuration of ROMS and, in a similar way to releasing dye in the ocean, can be used to trace the origins or destinations of water masses [e.g., *Macdonald et al.*, 2013]. In these numerical experiments, a passive dye tracer (representing the volume of shelf water) is released on the continental shelf with a concentration of 1 m^3 m^{-3} (1 m^3 of shelf water per m^3). This concentration is held constant on the continental shelf throughout the simulation so that waters on the continental shelf always have a passive tracer concentration of 1 m^3 m^{-3}. Off the continental shelf the dye tracer is initialized at 0 m^3 m^{-3} and allowed to evolve with time. As the simulation progresses through time the dye tracer is

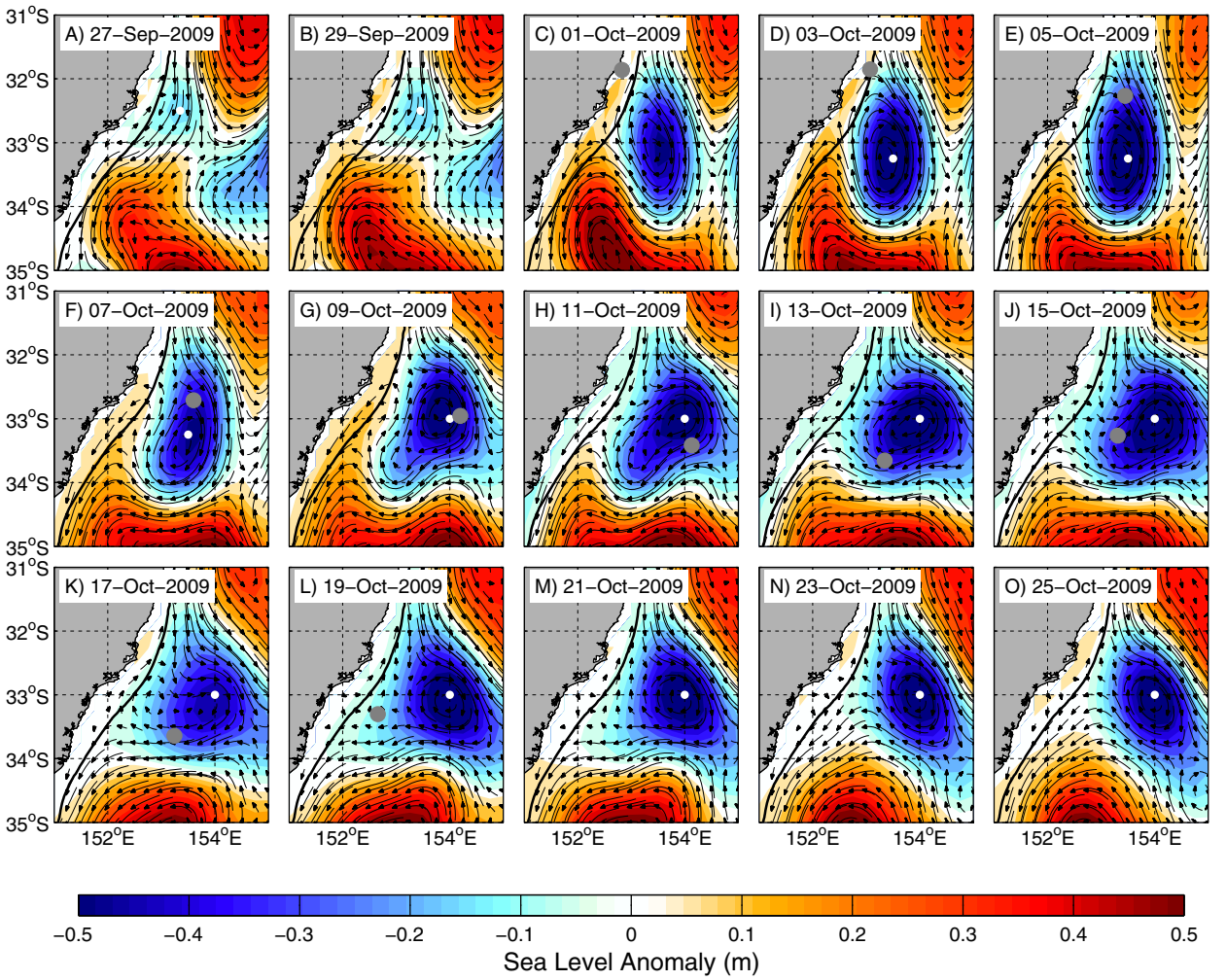

Figure 2. Surface geostrophic current estimated from sea level anomaly for the cyclonic eddy every 2 days from (a) 27 September 2009 to (o) 25 October 2009. The shading represent sea level anomaly, showing the cyclonic eddy with a depressed sea level. The white circle represents the center of the eddy as defined by the minimum sea level. The gray circle is the glider location at 00:00 h on that day.

advected and mixed throughout the model domain in a similar manner to other tracers (like temperature and salinity). The dye tracer has zero atmospheric flux and the lateral boundaries are treated in the same manner as other tracers in the model (radiative and nudging). The external nudging term in the boundary is set to 1 $m^3\ m^{-3}$ on the continental shelf and 0 $m^3\ m^{-3}$ off the shelf. The total volume of the dye tracer within the eddy on each day is used to quantify the volume of continental shelf waters entrained into the eddy. The volume change is calculated as the difference in volume from 1 day to the next and is expressed as Svedrups (Sv).

3. Results

In September 2009, prior to the development of the frontal eddy (cyclonic eddy with clockwise rotation), remotely sensed sea surface temperatures (SST) and altimetry show the East Australian Current (EAC) was flowing south at ~1 m s^{-1}, adjacent to the continental shelf. The frontal eddy studied in this paper formed around 1 October (Figure 2c) from a broad filament of cold water that upwelled off Seal Rocks (32.4°S; not shown). The formation of the eddy diverted the EAC offshore. The north-western flank of the eddy remained in close proximity (~60 km) to the continental shelf for a period of more than 30 days (Figure 2), directing a southeast flow of water off the shelf, which was subsequently entrained into the eddy. The eddy

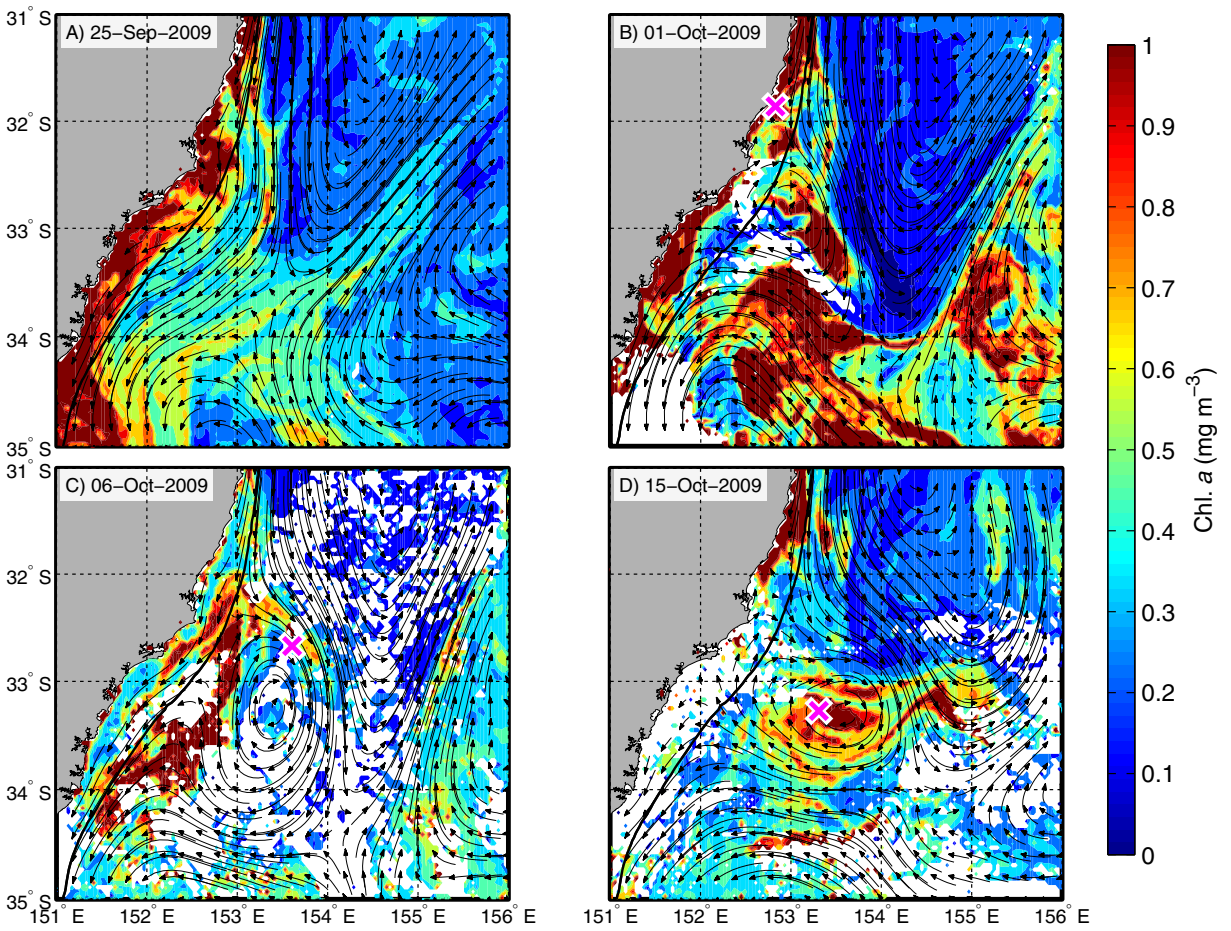

Figure 3. Surface chlorophyll *a* concentration (MODIS, Level 3) and geostrophic currents calculated from sea level anomaly for (a) 25 September, (b) 1 October, (c) 6 October, and (d) 15 October 2009. These days were selected due to the availability of images. The white sections indicate cloud cover and missing data. The position of the Slocum glider for the corresponding day is marked with a magenta cross.

began to move further offshore to the southeast on 8 October (Figures 2f and 2g) but remained in proximity to the shelf (<100 km) until it began to weaken and break up in early February 2010. The eddy existed for approximately 4 months (Table 1).

3.1. Eddy Entrainment Observations

MODIS satellite imagery shows a shelf enriched in chlorophyll *a* (25 September 2009; Figure 3a) prior to the formation of the eddy (1 October 2009; Figure 3b). The eddy formed on the continental shelf and entrained the enriched shelf water into the center of the eddy, visible as high chlorophyll *a* (Figure 3b). From the available satellite imagery, we observe the eddy continuing to entrain parcels of water throughout the study with a filament of high chlorophyll *a* biomass, entrained and transported around the northern sector of the eddy (Figure 3c).

The glider was deployed from Crowdy Head (32°S) on 1 October 2009 and made a 30 km cross-shelf transect immediately upstream of the cyclonic eddy (Figure 1). The shelf water was characterized by a stratified water column, with a surface mixed layer approximately 30–40 m deep. The surface mixed layer consisted of water temperatures of 18–19°C and a relatively high salinity (>35.5; Figure 4a, green box). The surface mixed layer had a high chlorophyll *a* biomass of 1–2 mg m^{-3} (Figure 4c). Intrusions of cooler and less saline slope water were evident in the bottom layers at the shelf edge, up to the 60 m isobath (Figure 4). We compared these characteristics of shelf water, to submerged parcels of water we subsequently observed within the eddy.

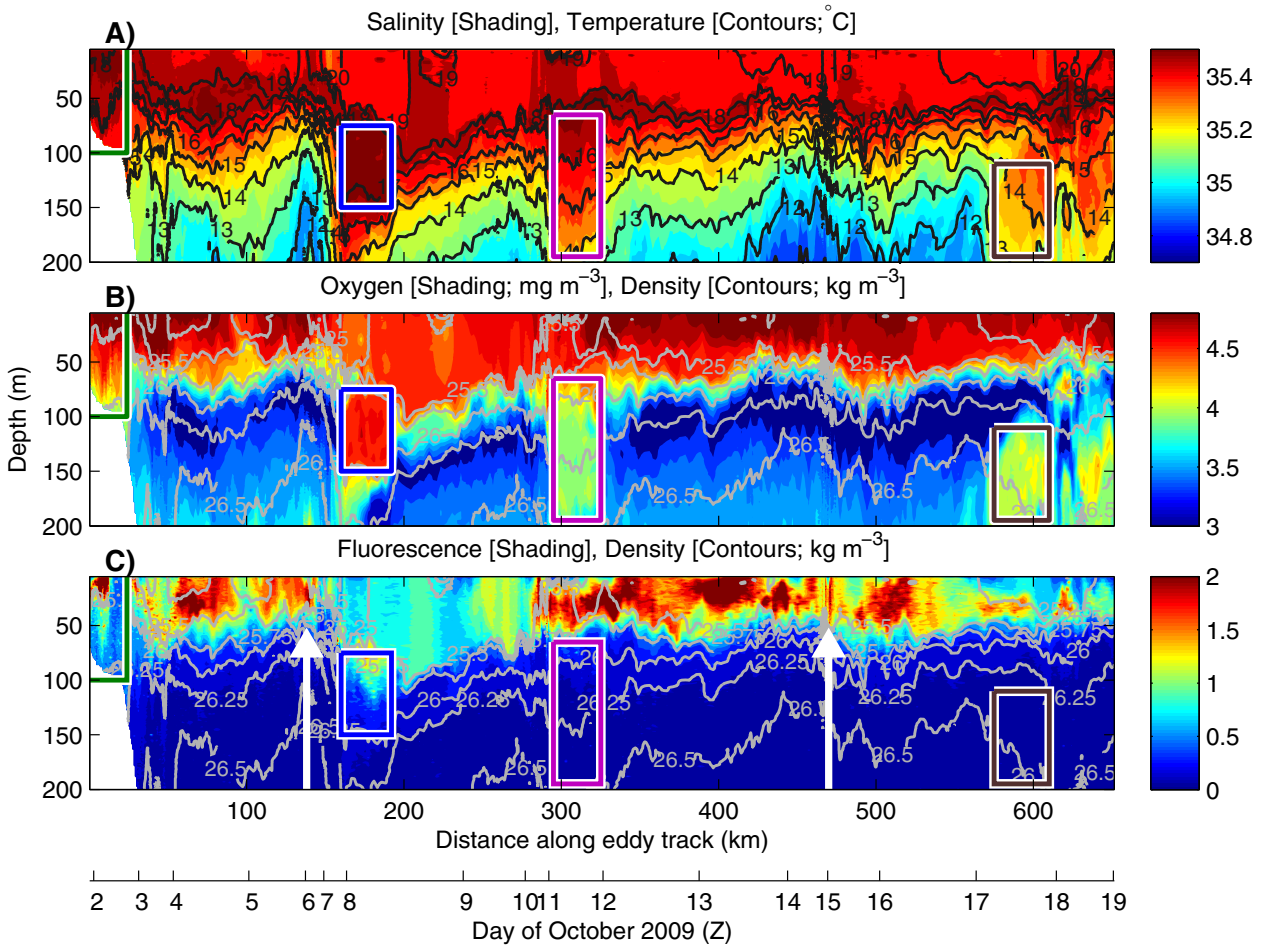

Figure 4. The glider transect showing (a) salinity (shaded) and temperature (contours), (b) oxygen (shaded) and density (contours), and (c) fluorescence (shaded) and density (contours). The distances on the *x* axis correspond to the distances marked in Figure 1. The date in October at 00:00 h is shown on a secondary axis below (c) and links to Figure 2. The four boxes correspond to the water masses in Figure 5: shelf water (green), submerged water masses 1, 2, and 3 (blue, purple, and brown, respectively). The white arrows correspond to the satellite overpass times for Figure 3c (left arrow) and Figure 3d (right arrow).

The glider left the shelf on the 3 October 2009 and entered the edge of the cyclonic eddy at approximately 50 km into the mission (4 October 2009). The glider never made it fully into the center of the cyclonic eddy, instead spiraling in toward the center, before making its way back out again. The water in the surface mixed layer of the eddy was slightly warmer (19°C) and less saline (35.4) than the shelf water (Figure 4a). Lifting of the isopycnals was evident within the eddy. The 15°C isotherm shoaled from 200 m depth near the edge of the eddy (150 km along transect; Figure 4a) to 100 m near the center (275 km along transect). This 100 m rise in the 15°C isotherm occurred within 10 days after the formation of the eddy (Figure 1), indicating an average shoaling of 10 m d^{-1}.

The glider observed high surface chlorophyll *a* at ~60–140 and 300–500 km along the track (Figure 4c; white arrows). These observations occur at coincident locations to where we observe elevated chlorophyll *a* in the MODIS imagery (magenta crosses in Figures 3c and 3d, respectively). The first observation (4–8 October; Figure 3c) is of a filament being entrained off the continental shelf at 32.5°S and wrapping around the northern perimeter of the eddy (magenta cross; Figure 3c). Also in this region of the eddy (Figure 2f), the glider sampled a patch of high oxygen (>4.5 mg m^{-3}) high salinity (>35.4) water that was observed just below the surface mixed layer at a depth of 75–150 m on 7 and 8 October 2009 (Figure 4b, blue box). This water mass had similar temperature and salinity properties to the shelf water observed previously by the glider (Figure 5, blue cluster). Peak chlorophyll *a* concentrations in this segment of the eddy were observed at the interface between the surface mixed layer and the submerged patch of water (Figure 4c, blue box).

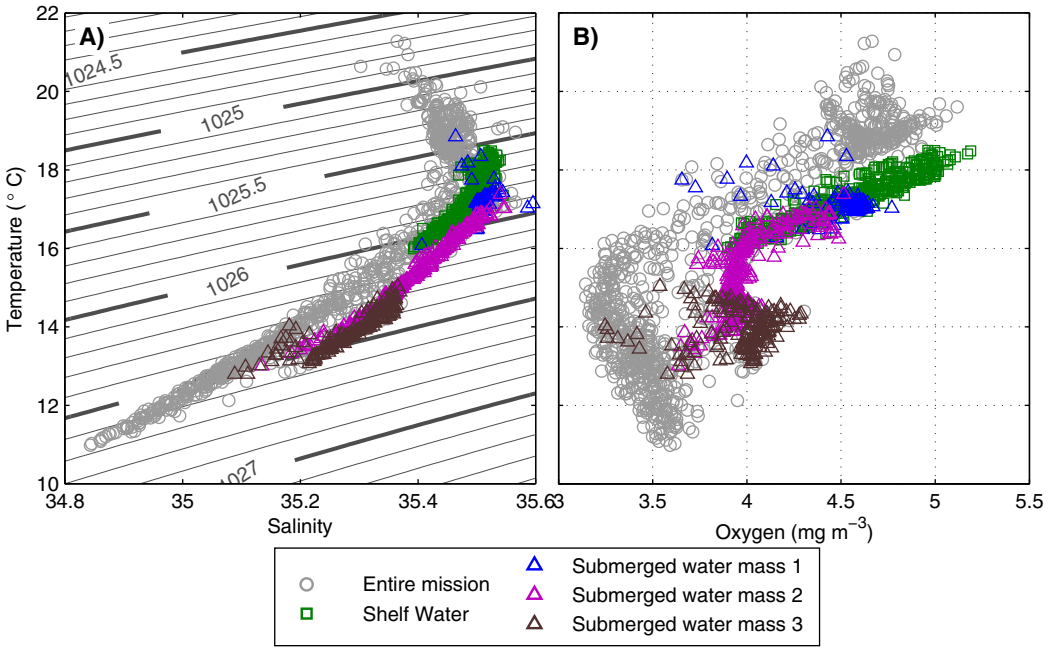

Figure 5. (a) Temperature/salinity and (b) temperature/oxygen diagrams showing all data (gray circles), shelf water (green squares), and three observations of entrained shelf water (blue, magenta, and brown triangles). The color of data points matches the colored boxes around water types from Figure 4.

3.2. Water Mass Mixing

The temperature-salinity diagram (Figure 5a) indicates that the eddy is predominately made up of Tasman Sea water which originated on the continental shelf. The glider sampled some Coral Sea waters near the surface, where the water was warmer than 18°C and lighter than 1025.4 kg m^{-3}. The oxygen concentration of the continental shelf waters along the glider transect (at 32°S) is elevated by 0.7 mg m^{-3} (Figure 5b, green cluster shifted right) relative to the bulk of the transect.

Two additional regions of cool, high oxygen (>3.8 mg m^{-3}) and high salinity (>35.2) water were observed in the southeastern and southwestern flanks of the eddy on 11–12 October 2009 and 17–19 October 2009 (Figures 4a and 4b; purple and brown boxes). These two filaments of entrained water have cooled by approximately 1°C relative to the rest of the shelf water (Figure 5a, purple/brown cluster shifted down). As a result, the two filaments are denser than the surrounding water and they therefore sink when they enter the eddy (Figure 4). The 0.7 mg m^{-3} of elevated oxygen is then clearly seen in the glider transect (Figure 4b; purple and brown boxes) and suggested recent contact with the surface.

We are not able to determine why two filaments of shelf water cooled by 1°C compared to the mean (Figure 5; magenta and brown clusters). It is most likely that the cooler waters have come from a shallow-depth coastal region where the water cooled prior to entrainment. Satellite observations (and model results shown below) indicated filaments of shelf water being entrained on the outer northwestern perimeter, and spiraling around the eddy. These spirals would appear as distinct patches of water as the glider crossed over them. This is consistent with our observations of the three water masses at the northern, southeastern and southwestern flanks of the cyclonic eddy, respectively (Figures 1 and 4). The glider was swept around the eddy, slowing down between 6–8 October and 13–17 October (Figure 1), resulting in a longer glider transect than the actual perimeter of the eddy. Using an average eddy radius of ~80 km (perimeter of ~502 km) from the first fortnight of the eddy census (Table 1), we can calculate the parcels of high oxygen water are approximately distributed 125 km apart, and the origin of the entrainment was estimated to be the northwestern flank of the eddy. Assuming a tangential velocity of ~0.5 m s^{-1} during the same period (Table 1) the parcels of high oxygen water were entrained approximately 2.6, 5.2, and 7.8 days prior to observation. For this eddy size and tangential velocity, the rotating period of the eddy is 12 days.

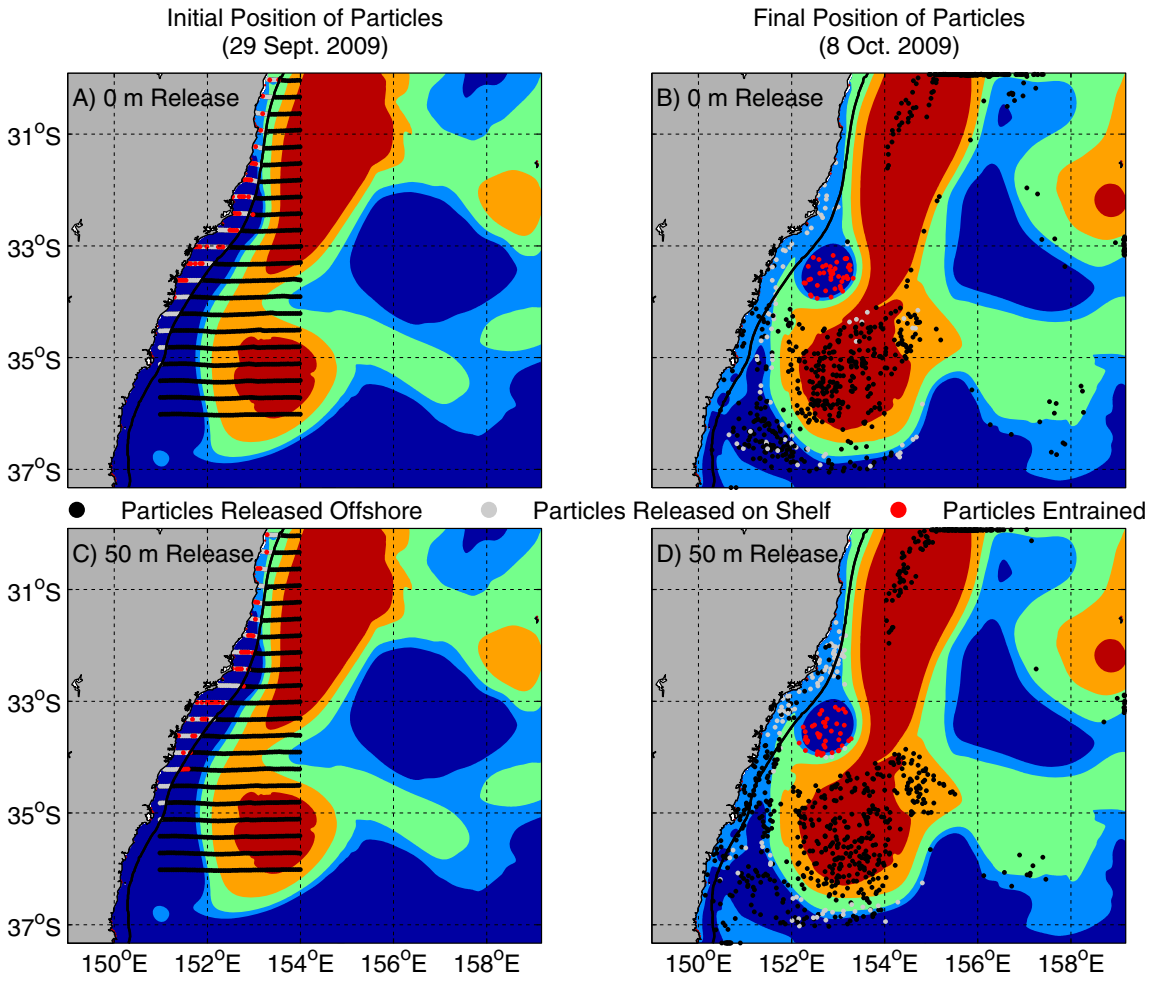

Figure 6. The initial (a and c; 29 September 2009) and final (b and d; 9 October 2009) position of released particles. The particles were released at two depths: (a and b) 0 m and (c and d) 50 m. The particles released on the shelf are colored gray and the particles entrained into the eddy on the 9 October 2009 are colored red. The remaining particles are black. Particles which leave the domain prior to the 9 October are located at their final location on the north, east, and south axes. The background color is modeled sea level anomaly (SLA), with the dark blue indicating a SLA of −0.85 m.

3.3. Entrainment Simulation

The numerical simulation of the cyclonic eddy clearly illustrates the process of entrainment observed in the oceanographic observations. The location of formation of the eddy on the shelf is consistent with altimetry observations, however the simulated eddy remains closer to the coast than altimetry suggests in the latter stages of the simulation. Within the simulation, the eddy forms on the 30 September off Port Stephens, on the western side of the EAC, consistent with satellite altimeter observations. The simulated eddy remains touching the shelf for the first week in agreement with oceanographic observations, however on the 8 October 2009, satellite observations (not shown) suggest the EAC starts to move eastward and the eddy began to move offshore. In the simulations, the EAC continues to flow southward and the eddy stays within 80 km of the shelf throughout the simulation. As a result, the model and SLA observations diverge from 9 October and therefore our quantification of entrainment was limited to 29 September to 9 October 2009.

Particle tracking experiments show the entrainment of shelf water occurs from along the entire coast (Figure 6) and the entrained water forms a spiral (Figure 7), similar to the observed MODIS chlorophyll *a* (Figures 3c). Particles were released both on and off the shelf on 22 September, yet particles released on the shelf (at 0 and 50 m) made up 92% ($n = 76$) of the particles which were in the eddy on the final day (Figures 6a and 6c). Particles from north and south of the eddy location, travelled up to 2° of latitude along the shelf, before being entrained into the eddy between 32°S and 33°S over the 10 days (Figure 7). Of the

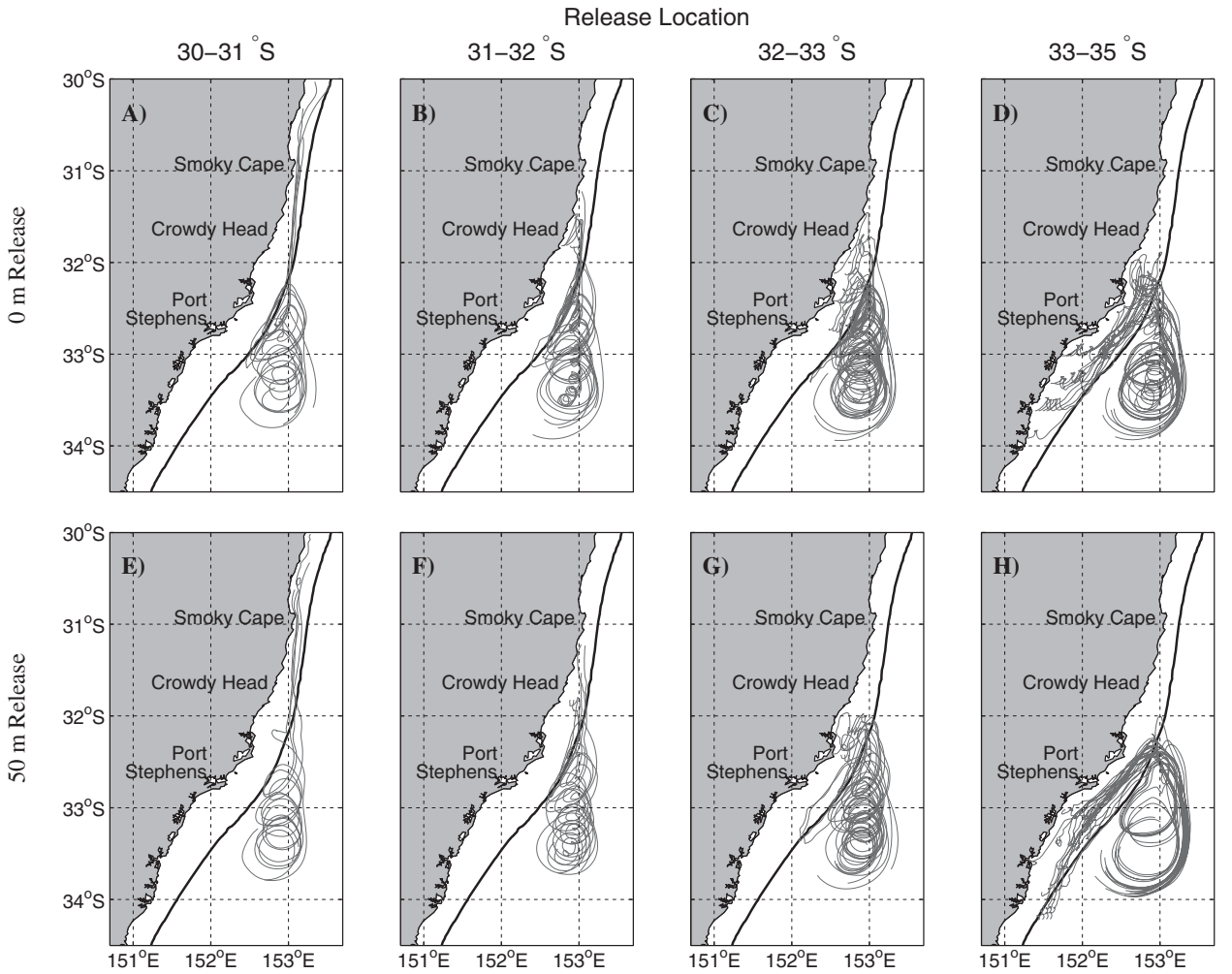

Figure 7. The tracks for the entrained particles are separated by their release location; (a and e) 30–31°S, (b and f) 31–32°S, (c and g) 32–33°S, and (d and h) 33–35°S. Those released at 0 m are shown in the top row, and those released at 50 m are shown on the bottom row. The thick black line indicates the shelf edge (200 m depth contour).

particles entrained (from 0 and 50 m), 30% originated from north of 32°S and 34% originated from south of 33°S. The remaining 36% were entrained from the shelf directly adjacent to the eddy location. Of those particles released at 0 and 50 m depth on the shelf, none leave the model domain, while 19% ($n = 24$) and 38% ($n = 41$) remain on the shelf (respectively) and 35% ($n = 43$) and 30% ($n = 33$) are entrained into the eddy. The remaining shelf particles (46% and 32%, respectively) are swept into the Tasman Sea (Figures 6b and 6d).

Similar to the observed sinking of entrained water masses in the glider observations, we used the particle tracking to examine the vertical movement of entrained particles. Particles released from 31°S to 33°S at 0 m sink during the simulation to an average depth of 20 m (Figure 8). Particles released south of 33°S, where the waters are cooler and denser, sank deeper, ending up at an average depth of 34 m. Particles released at 50 m show greater subduction. Particles from the south (33–35°S) sink to 75–115 m, however particles released from the north generally maintain their depth, ending up at a depth of 40–48 m.

Dye tracer experiments show that the surface waters (0–50 m depth) were of almost entirely (>95%) continental shelf origin (Figure 9 and Table 2) while at depths greater than 50 m, the eddy entrains waters from both the continental shelf and the open ocean. At 200 m depth, the eddy is about 60% continental shelf waters (not shown). The entrainment prior to the 9 October occurs at a rate of up to 2.2 Sv for the surface waters, calculated from the dye tracer (Table 2). Distance to the shelf was a critical factor in the entrainment

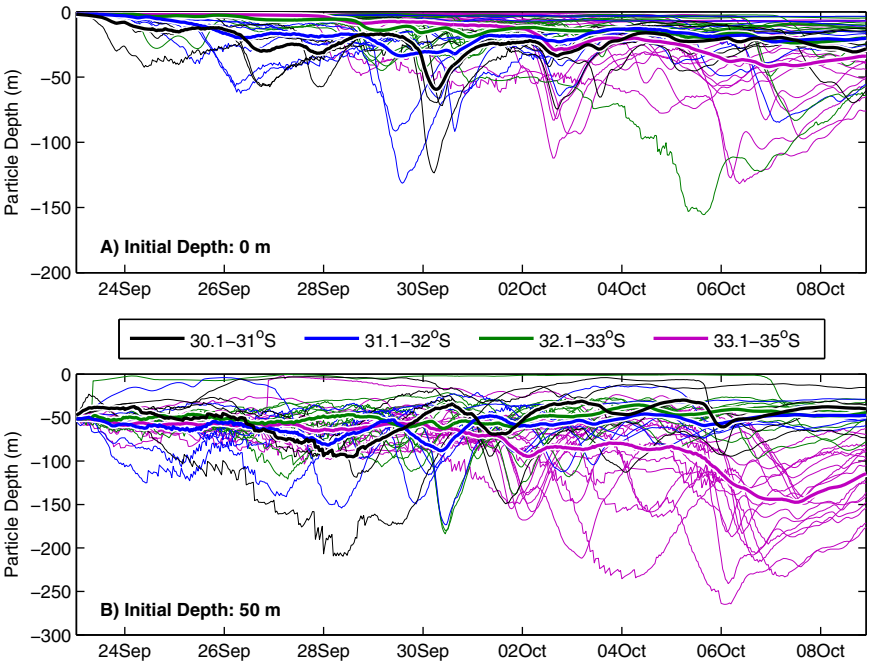

Figure 8. The depth evolution of the particles released at (a) 0 m and (b) 50 m and entrained into the frontal eddy is shown. The lines are colored by their release location; 30.1–31°S (black), 31.1–32°S (blue), 32.1–33°S (green), and 33.1–35°S (purple). The average depth of each release-location of particles is shown by the thicker line of corresponding color.

of coastal water. Entrainment occurred at 0.61 Sv (0–2.2 Sv) when the eddy was within 10 km of the continental shelf. However, when the eddy moved further offshore (4–6 October 2009), entrainment was reduced to 0.23 Sv (Table 2).

4. Discussion

The frequent formation of frontal eddies adjacent to enriched coastal waters, and their subsequent entrainment, is likely to play an important role in providing larval fish habitat [*Kasai and Kimura*, 2002; *Mackas et al*., 2005]. We reveal the process and magnitude for the entrainment of enriched coastal waters into a frontal eddy of the EAC from satellite observations, a glider deployment and a numerical simulation. Frontal eddies occur frequently within boundary current regions and often have lifetimes of only 1–3 weeks [*Lee et al*., 1991; *Mullaney and Suthers*, 2013]. Similar to this study however, other frontal eddies grow and persist for many months [*Glenn and Ebbesmeyer*, 1994].

4.1. Entrainment of Enriched Shelf Water

The glider observations show entrained parcels of water which occur progressively deeper in the water column through time. The observation of the first entrained parcel of water (Figure 4; blue box) occurs on 7 and 8 October at 75–150 m. This corresponds to the mean depth of the particles entrained from south of 33°S on the 9 October (75–115 m), indicating that this observed parcel of entrained water likely originated from a similar location. Due to the divergence of the observed and simulated eddy from 9 October (see section 3.3), we are unable to verify the location of the other two parcels of entrained water, which were observed on 11 and 17 October, respectively (Figure 4).

The depth of the entrained particles oscillated through time (Figure 8), and likely corresponded to a number of different processes within the eddy. Similar to the cyclonic eddy modeled by *Oke and Griffin* [2011] in the same region, the eddy in this study had a lean toward the coast [*Macdonald*, 2012] with particles on the eastern side of the eddy drawn deeper into the water column along-isopycnals, before being lifted back toward the surface. In addition, it is likely there was some cross-isopycnal movement, with downwelling in the eddy-center due to eddy-induced Ekman suction [*Gaube et al*., 2013] and more complex patterns of semigeostrophic vertical velocities which result in distinct signals in the eddy-center and outer periphery

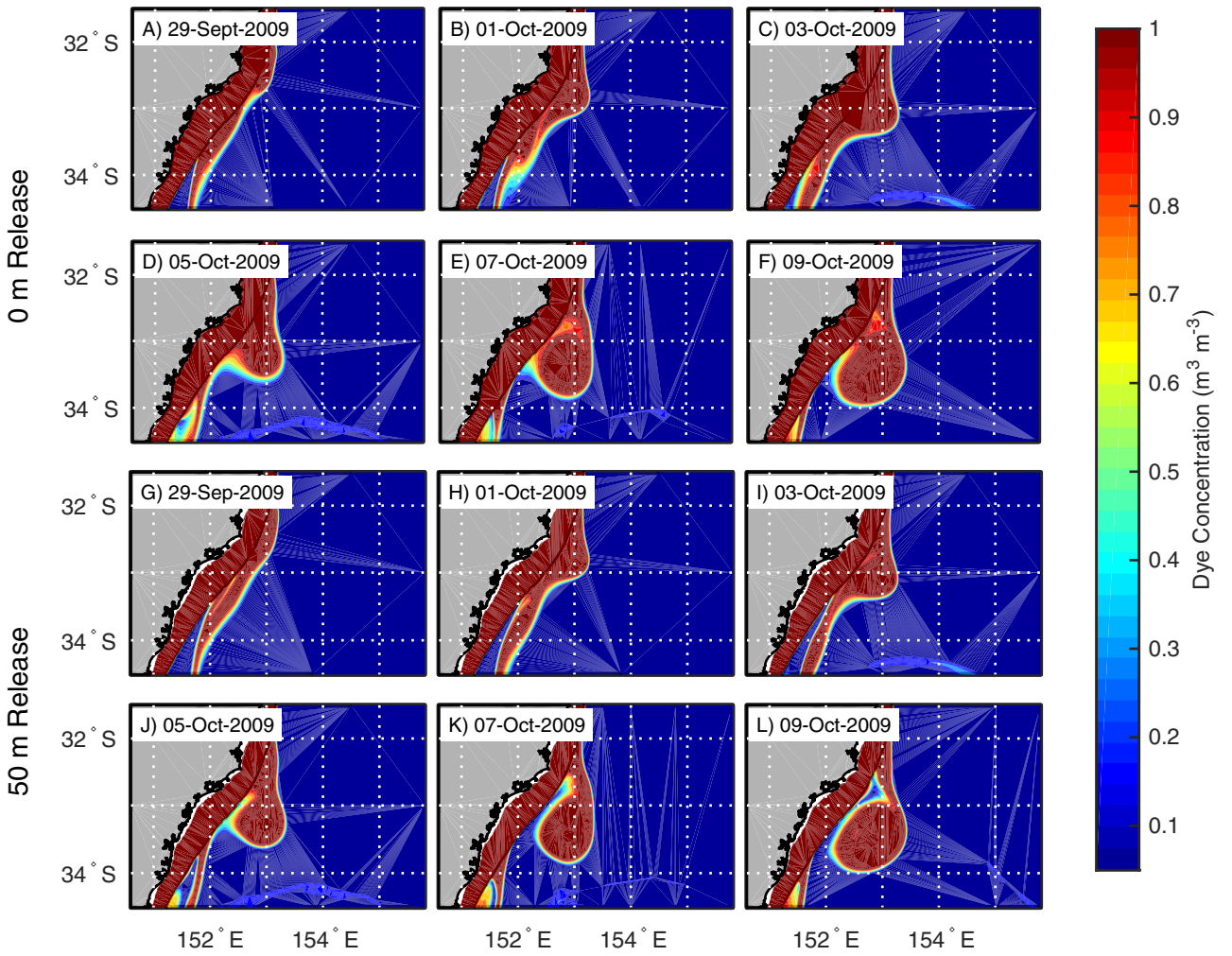

Figure 9. The use of a dye tracer quantifies the entrainment of shelf water at (top two rows) 0 m and (bottom two rows) 50 m. The dye is set to a value of 1 m^3 m^{-3} on the shelf (red) and 0 m^3 m^{-3} (blue) off the shelf. The concentration of the origin of the eddy waters is indicated by the color scale.

Table 2. Eddy Characteristics From the ROMS Eddy Simulation and Entrainment Metrics From the Dye Tracer Experiment[a]

			Modeled Eddy						Dye Tracer		
Area (km^2)	Δ Area (%)	Radius (km)	Δ Radius (%)	Distance (km)	V_t (cm s^{-1})	*Ro*	Vorticity ($\times 10^{-5}$ s^{-1})		Volume ($\times 10^9$ m^3)	Proportion (%)	Δ Volume (Sv)
2273		27		−12	61.05	0.14	−1.10	29 Sep	110	98	
3072	26	31	14	−12	63.40	0.13	−0.83	30 Sep	150	100	0.46
2936	−5	31	−2	1	63.50	0.13	−0.40	1 Oct	150	100	0
3350	12	33	6	3	63.01	0.12	−0.62	2 Oct	180	100	0.35
3783	11	35	6	8	61.13	0.12	−0.63	3 Oct	190	100	0.12
4091	8	36	4	12	53.97	0.09	−0.73	4 Oct	210	100	0.23
4710	13	39	7	16	53.84	0.09	−0.66	5 Oct	230	99	0.23
4962	5	40	3	20	65.03	0.1	−0.61	6 Oct	250	100	0.23
8976	45	53	26	7	63.22	0.07	−0.49	7 Oct	440	97	2.2
9665	7	55	4	6	60.60	0.07	−0.56	8 Oct	470	98	0.35
10,613	9	58	5	2	60.22	0.07	−0.59	9 Oct	510	97	0.46
12,009	12	62	6	0	56.55	0.06	−0.56	10 Oct	570	95	0.69

[a]Surface area of the eddy, radius of the eddy (assuming a circular eddy), and distance to the continental shelf from the eddy edge are calculated from the modeled sea level anomaly (SLA). A negative distance to the shelf indicates the eddy-edge is landward of the shelf break. Tangential velocity of the eddy (V_t), the Rossby Number (*Ro*), and the vorticity at the eddy-center are also shown. Dye volume is the total volume of dye tracer in the surface 50 m, and dye proportion is the proportion of the eddy (0–50 m) made up of shelf water. Daily entrainment volume is calculated as the mean daily Svedrups (Sv). Δ represents the change in the parameter from the previous day.

[*Nardelli*, 2013]. The parcels of entrained water observed by the glider (Figure 4) are consistent with what would be observed if the glider crossed over streamlines similar to the spiral formation of particles in the numerical experiments (Figure 7). The spiral pattern develops as the entrained water is continuously joining the north-western edge of the spinning eddy, thus forming a spiral as the eddy radius grows.

The continental shelf, adjacent to where the frontal eddy formed, is frequently enriched with nutrients [*Roughan and Middleton*, 2002], phytoplankton [*Everett et al*., 2014; *Armbrecht et al*., 2014], and larval fish [*Mullaney et al*., 2011] due to the onshore transport through the bottom boundary layer driven by the poleward flowing EAC [*Schaeffer et al*., 2013, 2014]. The frontal eddy formed from this enriched coastal water (Figure 9) and continued to entrain coastal water until it moved offshore around the 10 October 2009. By this time the eddy had entrained $570\times10^9 m^3$ of coastal water (Table 2). The eddy surface-area derived from altimetry shows that the eddy continued to grow until the 28 October 2009 (Table 1).

The adjacent EAC is the prevailing source of energy for the frontal eddy [*Macdonald*, 2012], with the subsequent eddy-rotation causing the nutricline to shoal, providing enrichment to sustain plankton. *Lee et al*. [1991] estimated that the density structure of a Gulf Stream frontal eddy shoaled by approximately 10 m d^{-1}, consistent with this study where the 15°C isotherm had shoaled from 200 m depth near the edge of the eddy to 100 m near the center within 10 days (Figure 4a).

4.2. Frontal Eddies as Offshore Nursery Habitats

Numerical simulations presented here show that coastal particles are transported into the region from as far as 2° of latitude north and south (±222 km) and subsequently entrained into the frontal eddy. This potential for particles to be advected northward (and southward) from downstream (upstream) into the vicinity of the eddy is in agreement with previous particle tracking experiments [*Roughan et al*., 2011] and biological sampling of larval fish communities [*Mullaney et al*., 2011]. *Mullaney et al*. [2011], for example, speculated that a suite of coastal larval fish which were found in the Tasman Front (the general region of this eddy), but whose source was unknown, had originated from the south via the northward flowing counter current [*Godfrey et al*., 1980].

During the first week of the eddy's life, it is entraining only shelf water, as shown by the surface dye concentrations reaching 100% (Table 2). Larval fish abundance on the continental shelf adjacent to the eddy ranges from 0.3 to 1.2 ind. m^{-3} [*Mullaney et al*., 2011]. The volume of shelf water entrained into the eddy (Table 2) suggests that $130–530\times10^9$ fish could be entrained into the eddy in the first week. Larvae from the continental shelf that are swept into the EAC are likely to be dispersed widely [*Roughan et al*., 2011] with lower survival and growth rates, however larvae entrained into frontal eddies may encounter more favorable conditions [*Okazaki et al*., 2003]. Larval fish sampled within an EAC frontal eddy had three orders of magnitude greater abundance of larval fish when compared to the shelf, and contained a greater proportion of older (postflexion) larvae which implies better survival [*Mullaney and Suthers*, 2013].

After formation (1–7 October), the frontal eddy moved up to 100 km off the shelf (Table 1), however the eddy and its associated plankton and larval fish were retained within the region, rather than being dispersed widely by the EAC. The frontal eddy moved south at a reduced velocity relative to the surrounding water. Upstream altimetry-derived geostrophic velocities (31°S, 154°S), calculated during the eddy lifetime (October 2009 to February 2010) shows the average southward velocity is 30 km d^{-1} (0.35 m s^{-1}). The frontal eddy had an average translational speed of 6 km d^{-1} (Table 1), indicating a fivefold decrease in transport. Similarly, *Mullaney and Suthers* [2013] describe an EAC frontal eddy that also had a approximately fivefold reduction in transport (0.08 m s^{-1}) over its 14 day life, relative to the surrounding EAC flow (0.2–0.5 m s^{-1}). The relatively short life of frontal eddies [*Lee et al*., 1991] and their reduced translational speed is sufficient to nurture fish through their pelagic larval duration, which can be as short as 9 days [*Lester et al*., 2007], and allow them to return to the coast as adults. The frontal eddy studied here moved westward toward the coast 8 weeks after formation (Table 1) allowing further opportunities for pelagic juvenile fish to return to the continental shelf. *Sponaugle et al*. [2005], for example, showed pulses of larval fish returning to the coast as Florida Current frontal eddies passed by the Florida Keys.

4.3. Frequency of Formation of Frontal Eddies

The sampling of the physical and biological structure of frontal eddies is often serendipitous, relying on equipment and personnel being in the right place at the right time. This study and other recent research [*Everett et al*., 2011; *Mullaney and Suthers*, 2013; *Matis et al*., 2014] has shown the planktonic and fisheries

potential of small frontal eddies, yet quantifying the frequency and duration of frontal eddies is critical to understanding their overall biological potential within a geographic region. This is difficult as they generally begin as smaller submesoscale features. Larger frontal eddies ($\gtrsim$80 km diameter) can be automatically censused and tracked using sea-surface height-anomalies [*Chelton et al*., 2011], which cannot easily resolve the more frequent smaller frontal eddies.

At the separation of the Gulf Stream off Florida, frontal eddies typically occur every 4–7 days and last 1–3 weeks [*Lee et al*., 1991; *Glenn and Ebbesmeyer*, 1994]. In the EAC separation zone, we have no data to quantify the number of frontal eddies of all sizes, however we do observe from satellite imagery small "billows" of cooler water being advected south [see *Everett et al*., 2011, Figure 2] on approximately weekly time scales [*Mullaney and Suthers*, 2013]. Due to their oft small size at formation, frontal eddies are not always identified immediately if at all. By the time they are identified in altimetry products the frontal eddies may have finished their entrainment and moved away from the coast. Products with improved horizontal resolution such as radar systems will improved the quantification of these important features in the future [*Kim*, 2010].

5. Concluding Remarks

The frontal eddy observed in this study encroached onto the continental shelf for an extended period of time. The cyclonic rotation provided a mechanism for the entrainment of biologically rich water from the continental shelf into the main body of the eddy. This could be a pathway by which cyclonic eddies associated with the EAC may be seeded with larval fish and their zooplankton prey. Particle tracking experiments show the eddy entrained water which originated from over 200 km away, but that all entrainment occurred from the adjacent shelf, north-west of the eddy center.

A key question which remains unanswered is what are the oceanographic conditions which result in entrainment? This study has quantified the volume of entrainment from a single frontal eddy. Due to the modeled eddy not moving away from the coast in this study, it is still unclear at what stage entrainment starts and ends, however it was clear that entrainment was reduced when the eddy moved further away from the coast (Table 2). Even a short duration eddy ($<$1 month) would be sufficient for plankton to grow and for fish larvae to develop before swimming back to the coast. The results presented here show that frontal eddies associated with boundary currents can have significant implications for local fisheries by entraining enriched shelf water and providing additional nearshore habitat for growth and survival.

Acknowledgments

J.D.E. was jointly supported by DP120100728 held by IMS and funding from the NSW Science Leveraging Fund. Glider, Altimetry, and MODIS-Chlorophyll data are freely available from the Australian Integrated Marine Observing System (IMOS; http://www.imos.org.au), an initiative of the Australian Government being conducted as part of the National Collaborative Research Infrastructure Strategy and the Super Science Initiative. ROMS output data may be requested by contacting the authors. Special mention to IMOS-ANFOG and Ben Hollings for their support of the glider program. We also acknowledge the MODIS mission scientists and associated NASA personnel for the production of the data used in this research effort. We thank the Editor, Professor Edward Barton and two anonymous reviewers, whose comments greatly improved the manuscript. This is manuscript 145 from the Sydney Institute of Marine Science.

References

Armbrecht, L. H., M. Roughan, V. Rossi, A. Schaeffer, P. L. Davies, A. M. Waite, and L. K. Armand (2014), Phytoplankton composition under contrasting oceanographic conditions: Upwelling and downwelling (Eastern Australia), *Cont. Shelf Res.*, *75*, 54–67.

Baird, M. E., I. M. Suthers, D. A. Griffin, B. Hollings, C. Pattiaratchi, J. D. Everett, M. Roughan, and M. A. Doblin (2011), The effect of surface flooding on the physical-biogeochemical dynamics of a warm-core eddy off southeast Australia, *Deep Sea Res., Part II*, *58*(5), 592–605.

Chelton, D. B., M. G. Schlax, and R. M. Samelson (2011), Global observations of nonlinear mesoscale eddies, *Prog. Oceanogr.*, *91*(2), 167–216.

Deng, X., D. A. Griffin, K. R. Ridgway, J. Church, W. Featherstone, N. White, and M. Cahill (2011), Satellite altimetry for geodetic, oceanographic and climate studies in the Australian region, in *Coastal Altimetry*, edited by S. Vignudelli et al., pp. 473–508, Springer, Berlin.

Everett, J. D., M. E. Baird, and I. M. Suthers (2011), Three-dimensional structure of a swarm of the salp *Thalia democratica* within a cold-core eddy off southeast Australia, *J. Geophys. Res.*, *116*, C12046, doi:10.1029/2011JC007310.

Everett, J. D., M. E. Baird, and I. M. Suthers (2012), An avenue of eddies: Quantifying the biophysical properties of mesoscale eddies in the Tasman Sea, *Geophys. Res. Lett.*, *39*, L16608, doi:10.1029/2012GL053091.

Everett, J. D., M. E. Baird, M. Roughan, I. M. Suthers, and M. A. Doblin (2014), Relative impact of seasonal and oceanographic drivers on surface chlorophyll a along a Western Boundary Current, *Prog. Oceanogr.*, *120*, 340–351, doi:10.1016/j.pocean.2013.10.016.

Flather, R. (1976), A tidal model of the northwest European continental shelf, *Mem. Soc. R. Sci. Liege*, *6*(10), 141–164.

Gaube, P., P. G. Strutton, D. B. Chelton, and M. J. Behrenfeld (2013), Satellite observations of chlorophyll, phytoplankton biomass and Ekman pumping in nonlinear mesoscale eddies, *J. Geophys. Res. Oceans*, *118*, 6349–6370, doi:10.1002/2013JC009027.

Glenn, S. M., and C. C. Ebbesmeyer (1994), Observations of Gulf Stream frontal eddies in the vicinity of Cape Hatteras, *J. Geophys. Res.*, *99*(C3), 5047–5055, doi:10.1029/93JC02787.

Godfrey, J. S., G. R. Cresswell, T. J. Golding, and A. F. Pearce (1980), The separation of the East Australian Current, *J. Phys. Oceanogr.*, *10*(3), 430–440.

Govoni, J. J., J. A. Hare, E. D. Davenport, M. H. Chen, and K. E. Marancik (2010), Mesoscale, cyclonic eddies as larval fish habitat along the southeast United States shelf: A Lagrangian description of the zooplankton community, *ICES J. Mar. Sci.*, *67*(3), 403–411.

Govoni, J. J., J. A. Hare, and E. D. Davenport (2013), The distribution of larval fishes of the Charleston gyre region off the southeastern United States in winter shaped by mesoscale, cyclonic eddies, *Mar. Coastal Fish.*, *5*(1), 246–259.

Kasai, A., and S. Kimura (2002), Entrainment of coastal water into a frontal eddy of the Kuroshio and its biological significance, *J. Mar. Syst.*, *37*(1), 185–198.

Kim, S. Y. (2010), Observations of submesoscale eddies using high-frequency radar-derived kinematic and dynamic quantities, *Cont. Shelf Res.*, *30*(15), 1639–1655.

Kim, S. Y., et al. (2011), Mapping the U.S. West Coast surface circulation: A multiyear analysis of high-frequency radar observations, *J. Geophys. Res.*, *116*, C03011, doi:10.1029/2010JC006669.
Kimura, S., A. Kasai, T. Sugimoto, J. H. Simpson, and J. V. S. Cheok (1997), Biological productivity of meso-scale eddies caused by frontal disturbances in the Kuroshio, *ICES J. Mar. Sci.*, *54*(2), 179–192.
Lee, T. N. (1975), Florida current spin-off eddies, *Deep Sea Res. Oceanogr. Abstr.*, *22*(11), 753–765.
Lee, T. N., J. A. Yoder, and L. P. Atkinson (1991), Gulf Stream frontal eddy influence on productivity of the southeast US continental shelf, *J. Geophys. Res.*, *96*(C12), 22,191–22,205, doi:10.1029/91JC02450.
Lester, S. E., B. I. Ruttenberg, S. D. Gaines, and B. P. Kinlan (2007), The relationship between dispersal ability and geographic range size, *Ecol. Lett.*, *10*(8), 745–758.
Logerwell, E. A., and P. E. Smith (2001), Mesoscale eddies and survival of late stage Pacific sardine (*Sardinops sagax*) larvae, *Fish. Oceanogr.*, *10*(1), 13–25.
Macdonald, H. S. (2012), Numerical modelling of mesoscale eddies in the Tasman Sea, PhD thesis, Univ. of N. S. W., Sydney, Australia. [Available at http://handle.unsw.edu.au/1959.4/52532.]
Macdonald, H. S., M. Roughan, M. E. Baird, and J. Wilkin (2013), A numerical modelling study of the East Australian Current encircling and overwashing a warm-core eddy, *J. Geophys. Res. Oceans*, *118*, 301–315, doi:10.1029/2012JC008386.
Mackas, D. L., M. Tsurumi, M. D. Galbraith, and D. R. Yelland (2005), Zooplankton distribution and dynamics in a North Pacific Eddy of coastal origin. II: Mechanisms of eddy colonization by and retention of offshore species, *Deep Sea Res., Part II*, *52*(7–8), 1011–1035.
Marchesiello, P., J. C. McWilliams, and A. Shchepetkin (2001), Open boundary conditions for long-term integration of regional oceanic models, *Ocean Modell.*, *3*(1–2), 1–20.
Matis, P. A., W. F. Figueira, I. M. Suthers, J. Humphries, A. Miskiewicz, R. A. Coleman, B. P. Kelaher, and M. D. Taylor (2014), Cyclonic entrainment? The ichthyoplankton attributes of three major water mass types generated by the separation of the East Australian Current, *ICES J. Mar. Sci.*, *71*(7), 1696–1705.
Mellor, G. L., and T. Yamada (1982), Development of a turbulence closure-model for geophysical fluid problems, *Rev. Geophys.*, *20*(4), 851–875.
Mullaney, T. J., and I. M. Suthers (2013), Entrainment and retention of the coastal larval fish assemblage by a short-lived, submesoscale, frontal eddy of the East Australian Current, *Limnol. Oceanogr. Methods*, *58*(5), 1546–1556.
Mullaney, T. J., A. G. Miskiewicz, M. E. Baird, P. T. P. Burns, and I. M. Suthers (2011), Entrainment of larval fish assemblages from the inner shelf into the East Australian Current and into the western Tasman Front, *Fish. Oceanogr.*, *20*(5), 434–447.
Nakata, H., S. Kimura, Y. Okazaki, and A. Kasai (2000), Implications of meso-scale eddies caused by frontal disturbances of the Kuroshio Current for anchovy recruitment, *ICES J. Mar. Sci.*, *57*(1), 143–152.
Nardelli, B. B. (2013), Vortex waves and vertical motion in a mesoscale cyclonic eddy, *J. Geophys. Res. Oceans*, *118*, 5609–5624, doi:10.1002/jgrc.20345.
Okazaki, Y., H. Nakata, and S. Kimura (2002), Effects of frontal eddies on the distribution and food availability of anchovy larvae in the Kuroshio Extension, *Mar. Freshwater Res.*, *53*, 403–410.
Okazaki, Y., H. Nakata, S. Kimura, and A. Kasai (2003), Offshore entrainment of anchovy larvae and its implication for their survival in a frontal region of the Kuroshio, *Mar. Ecol. Prog. Ser.*, *248*, 237–244.
Oke, P. R., and D. A. Griffin (2011), The cold-core eddy and strong upwelling off the coast of New South Wales in early 2007, *Deep Sea Res., Part II*, *58*(5), 574–591.
Ridgway, K. R., R. C. Coleman, R. J. Bailey, and P. Sutton (2008), Decadal variability of East Australian Current transport inferred from repeated high-density XBT transects, a CTD survey and satellite altimetry, *J. Geophys. Res.*, *113*, C08039, doi:10.1029/2007JC004664.
Roughan, M., and J. H. Middleton (2002), A comparison of observed upwelling mechanisms off the east coast of Australia, *Cont. Shelf Res.*, *22*(17), 2551–2572.
Roughan, M., H. S. Macdonald, M. E. Baird, and T. M. Glasby (2011), Modelling coastal connectivity in a Western Boundary Current Seasonal and inter-annual variability, *Deep Sea Res., Part II*, *58*(5), 628–644.
Schaeffer, A., M. Roughan, and B. D. Morris (2013), Cross-shelf dynamics in a western boundary current regime: Implications for upwelling, *J. Phys. Oceanogr.*, *43*(5), 1042–1059.
Schaeffer, A., M. Roughan, and J. E. Wood (2014), Observed bottom boundary layer transport and uplift on the continental shelf adjacent to a western boundary current, *J. Geophys. Res. Oceans*, *119*, 4922–4939, doi:10.1002/2013JC009735.
Shannon, L. V., P. Schlittenhardt, and S. A. Mostert (1984), The Nimbus-7 CZCS experiment in the Benguela current region off Southern Africa, February 1980. 2: Interpretation of imagery and oceanographic implications, *J. Geophys. Res.*, *89*(D4), 4968–4976.
Shchepetkin, A. F., and J. C. McWilliams (2003), A method for computing horizontal pressure-gradient force in an oceanic model with a nonaligned vertical coordinate, *J. Geophys. Res.*, *108*(C3), 3090, doi:10.1029/2001JC001047.
Shchepetkin, A. F., and J. C. McWilliams (2005), The regional oceanic modeling system (ROMS): A split-explicit, free-surface, topography-following-coordinate oceanic model, *Ocean Modell.*, *9*(4), 347–404.
Sponaugle, S., T. Lee, V. Kourafalou, and D. Pinkard (2005), Florida Current frontal eddies and the settlement of coral reef fishes, *Limnol. Oceanogr. Methods*, *50*(4), 1033–1048.
Yoder, J. A., L. P. Atkinson, T. N. Lee, H. H. Kim, and C. R. McClain (1981), Role of gulf-stream frontal eddies in forming phytoplankton patches on the outer southeastern shelf, *Limnol. Oceanogr.*, *26*(6), 1103–1110.
Zhang, H. M., R. W. Reynolds, and J. J. Bates (2006), Blended and gridded high resolution global sea surface wind speed and climatology from multiple satellites: 1987–present, paper presented at 86th AMS Annual Meeting, Atlanta, 29 Jan to 2 Feb.